THE POST VIENNA CONFERENCE ON GEOTEXTILES
SINGAPORE, 1987

57

STABILITY OF STEEP CLAY EMBANKMENTS REINFORCED WITH A NON-WOVEN GEOTEXTILE

YAMAUCHI, H
PENTA-OCEAN CONSTRUCTION CO LTD
JAPAN
TATSUOKA, F
INSTITUTE OF INDUSTRIAL SCIENCE, UNIVERSITY OF TOKYO
JAPAN
NAKAMURA, K; TAMURA, Y
TOKYU CONSTRUCTION CO LTD
JAPAN
IWASAKI, K
MITSUI PETROCHEMICAL INDUSTRIES LTD
JAPAN

1. INTRODUCTION

The effects of non-woven geotextile reinforcement on the stability o four clay test embankments are examined based on their performance. Thi paper is an extension of the previous two papers (1), (2).

Reinforcement for nearly saturated cohesive soils should has an abilit to drain the soil, which steel reinforcement and polymer grid do not have In spite of its low tensile stiffness, non-woven geotextiles may be use for reinforcing clay embankments because of its high ability to drain th soil (1), (2). Note that in order to overcome its largest drawback of mos existing non-woven geotextiles (i.e., low tensile stiffness), recently non-woven geotextile sheet reinforced with a low-cost material having a hig initial tensile stiffness has become available (3). In this paper, it wil be shown that even using a usual non-woven geotextile having a relativel low tensile stiffness, very steep slopes (1 : 0.2 ~0.3 ; horizontal to vertica of medium to low height (less than 5.5m) clay embankments can be effectivel reinforced.

2. CLAY TEST EMBANKMENTS

Three of the four test embankments, I, II and III were constructed at th same site (Fig.1), while the other one was constructed at another site (3

	Embankment I		Embankment II		Embankment III
Slope	R	L	R	L	R, L, B
L_B	2.0	2.0	2.8	3.8	2.5, 5.0
L_T	2.0	2.0	1.24	2.24	2.5, 5.0
L_1	7.6		10.0		12.2
L_2	22.0		23.4		21.15
L_3	6.0		6.48		10.0
L_4	10.0		12.0		10.55
H	4.0		5.2		5.5
ΔH	0.4	0.8	0.4	0.4	0.5
S	0.2		0.3		0.2
a	2.5		4.0		
b	5.0		4.0		UNIT:m
c	2.5		4.0		

MASS PER UNIT AREA OF NON-WOVEN GEOTEXTILE

$M(g/m^2)$	400[a]	300[a]	300[a]

a. NOMINAL

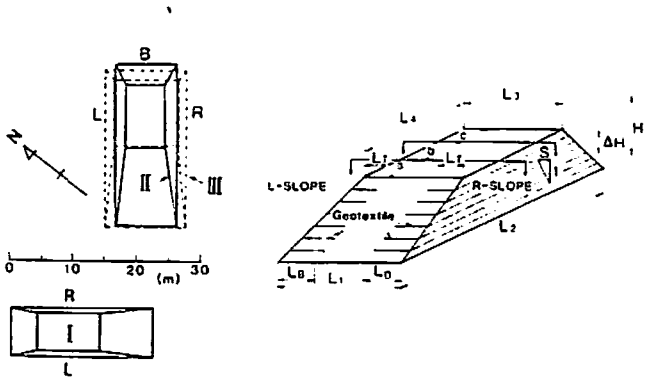

Fig.1. Initial dimensions of test embankments constructed at Chiba Experiment Station, Institute of Industrial Science, Univ. of Tokyo.

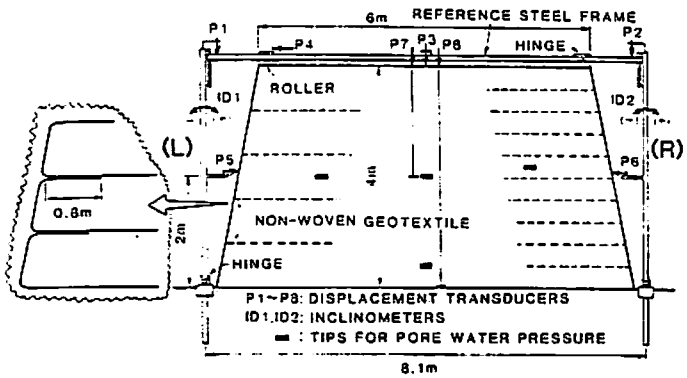

Fig.2. Cross-section of Embankment I.

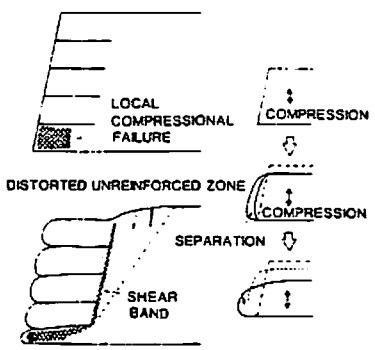

Fig.3. Local compressional failure of soil and associated sliding failure.

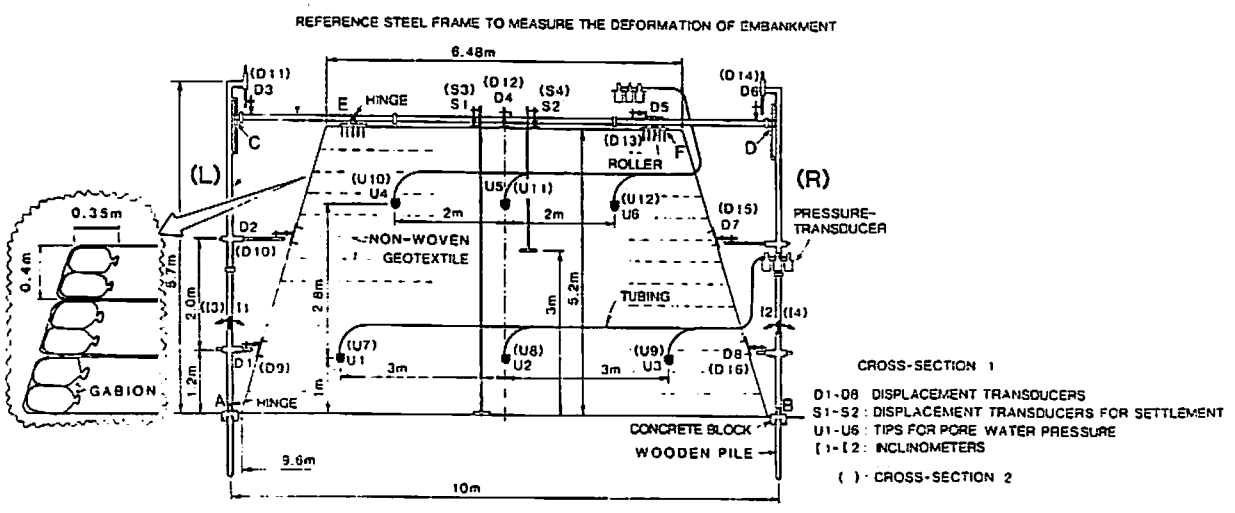

Fig.4. Cross-section of Embankment II.

Table 1. Properties of soil used for Embankments Ⅰ, Ⅱ and Ⅲ.

Intact

w_n≒120%, ρ_d≒0.52g/cm³, w_l=168%, w_p=115%, PI=53, G_s=2.899, D_{50}=14.5μm

clay content (<5μm)=29%, silt content (5~74μm)=63%, sand content (>74μm)=8%

cone penetration resistance : q_c=10~30kgf/cm²

$\overline{CU}$ triaxial compression test ; ϕ'=29.6°, c'=0.07kgf/cm²

$\overline{CU}$ triaxial extension test ; ϕ'=31.2°, c'=0.09kgf/cm²

Embankment Ⅰ

at filling (June 1982) : w≒100%

at demolishing (Oct. 1985) : w≒93% [a], S_r≒85% [a], ρ_d≒0.69g/cm³ [a], q_c=4~6kgf/cm²

$\overline{CU}$ triaxial compression test ; ϕ'=35~37°, c'=0.

[a] Averaged excluding near the crest.

Embankment Ⅱ

at filling (Oct. 1985) : w≒120%, S_r≒90%, ρ_d≒0.55~0.65g/cm³, q_c=5~10kgf/cm² [b], 2~7kgf/cm³ [c],

[b] For mechanically compacted layers.

[c] For manually compacted layers about 1m next to the slope face.

at demolishing (Oct. 1986) : w=104~119% [a], S_r≒78~85% [a], ρ_d=0.60~0.67g/cm³

$\overline{CU}$ triaxial compression test ; ϕ=39° at large strains.

Embankment Ⅲ

at filling (Oct. 1985) : w≒110%, S_r≒85%, ρ_d≒0.6g/cm³

Table 2. Mechanical and hydraulic properties of non-woven geotextile.

Fiber density ρ_f (g/cm³) = 0.31

Fiber diameter d_f (mm) = 0.40

Mass per unit area as measured μ (g/m²) ≒ 400 (nominal = 300g/m²)

Unstressed thickness (mm) = 4

Permeability in plane (cm/sec) [a] ≒ 2×10^{-1}~3×10^{-2}

Friction angle at interface

with Kanto loam under water (in degree) [a] = 28~37 [c]

Force per unit width at 15% elongation $\alpha_{0.15}$ (tf/m) [b] = $0.435 + 0.00675\sigma_0$

Force per unit width at peak α_f (tf/m) [b] = $1.5 + 0.017\sigma_0$

Poisson ratio ν_g [d] = 0.0

a) For normal stress σ_0 (tf/m²) = 0~32.

b) For normal stress σ_0 (tf/m²) = 0~20.

c) These values are similar to the angle of internal friction at large strains of Kanto loam.

d) The value when compressed in the direction normal to the plane.

These are as follows:

Embankment I (Fig.2), constructed in June 1982, has two test steep slopes, being 1:0.2, and a height of 4.0m. The flat slope faces were made and they were wrapped around with non-woven geotextile round the soil at the face. Eventually, this face construction method was found to be time-consuming. In addition, as schematically shown in Fig.3, the confinement of the soil next to the slope face was lost when the soil was compressed vertically, triggering further compression of the soil. This face construction method is not recommended to use in practice.

Embankment II (Fig.4) was constructed in March 1984. The two test slopes had a slope of 1:0.3 and a height of 5.2m. Based on the poor performance of the left-hand slope face of Embankment I, two layers of gabions, which were made of a non-woven geotextile and filled with the clay as used for the construction of the embankment, were placed at the shoulder of each previous layer of the slope before placing the soil layer. The gabions were well compressed vertically when placed so that they will not be compressed by further filling and loading. In actuality, the gabions helped better compaction of the soil near the slope faces and also prevented its local failure during and also after filling. Since the gabions were wrapped with the geotextile, the geotextile deteriorated by having been exposed to strong ultraviolet light in summer. With some measures to avoid this problem, this face construction method using gabions may be used in actual construction projects. During eight days in October 1985, about 70m^3 of water was supplied from a pond made on the crest to critically evaluate its stability. Subsequently, after observing its performance for about one more year, it was demolished in October 1986. In this paper, the behavior of this embankment during the water supply and the subsequent period will be reported in detail.

The other two embankments, Embankment III and Kami-onda Embankment, are described in detail in the companion paper (3). All the embankments were made using the same kind of volcanic ash clay, called Kanto loam (Table 1). This soil is one of problematic soils because of its high sensitivity of 4~5; during construction works, this soil is considerably weakened by remolding due to its high natural water content of the order of 120~130%. Similar kind of problematic clayey soils may be found in many other places in Japan as well as in countries having active volcanoes.

Each soil layer was compacted to a 25-40cm thickness using compaction

plant. Within about 1m of the slope face, manual compaction was used excep Embankment Ⅲ. For Embankment Ⅱ, light compaction plant was used near th slope faces as well.

For all the embankments, the same kind of spun-bondeed (needle-punched 100% polypropylene non-woven geotextile was used, while the thickness i slightly different among different embankments (Fig.1 and Table 2 Horizontal planar sheets were placed as shown in Figs.1-4. After having bee: used as a reinforcing material in Embankments Ⅰ and Ⅱ for 30 or 40 months the geotextile was sampled from the interior of the embankments when the: were demolished. Their mechanical and hydraulic properties were carefull: evaluated and were found to have not changed at any rate from those o: the fresh geotextile (4).

The non-woven geotextile was used for the following three purposes:
(1) To allow better compaction of the fill. By placing the geotextile sheet: horizontally with a vertical spacing, each relatively thin soil layer i: inevitably well compacted. By tensile resistances of the geotextile horizontal tensile strains in the soil when vertically compacted ar: restrained, resulting in better compaction. Possible excess pore wate: pressure induced during compaction and further filling is effectivel: drained. Compaction plant can be used near the face, supported by th: underlying reinforced soil layers.
(2) To drain water quickly out of the embankment in order to maintain a sufficient amount of suction (negative pore water pressure) and to prevent an increase in positive pore water pressure during heavy rainfall.
(3) To tensile-reinforce embankments. This includes the prevention of development of vertical cracks; the possitive water pressure developed ir cracks during heavy rainfall decreases considerably the stability of slope: by softening the soil and applying a horizontal load to the slope.

As shown in Figs.1-4, the vertical spacing and the length of the geotextile sheets were varied among the slopes. It was found that a vertical spacing of 80cm without using any measures for confining the soil near the face as used in the left-hand slope of Embankment Ⅰ (Fig.2) is too large; i.e., as reported in (1), (2), a large displacement of the slope took place triggered by a large local compression in the lowest soil layer (see also Fig.3).

For the right-hand slope of Embankment Ⅱ (Fig.4), the length of the non-woven geotextile reinforcement was made very small as compared to the values used in the present practice. The reasons are as follows.
(a) When compared to the strip reinforcement of steel, the ratio = "the

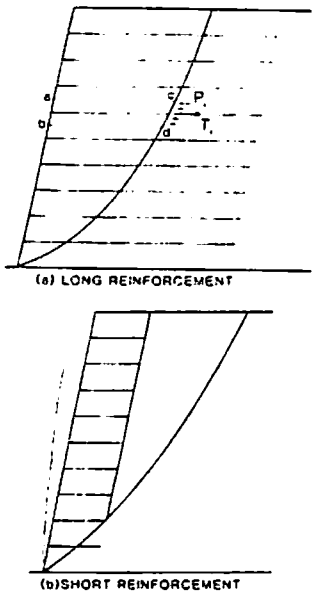

Fig.5.

Possible failure mechanisms in reinforced slopes.

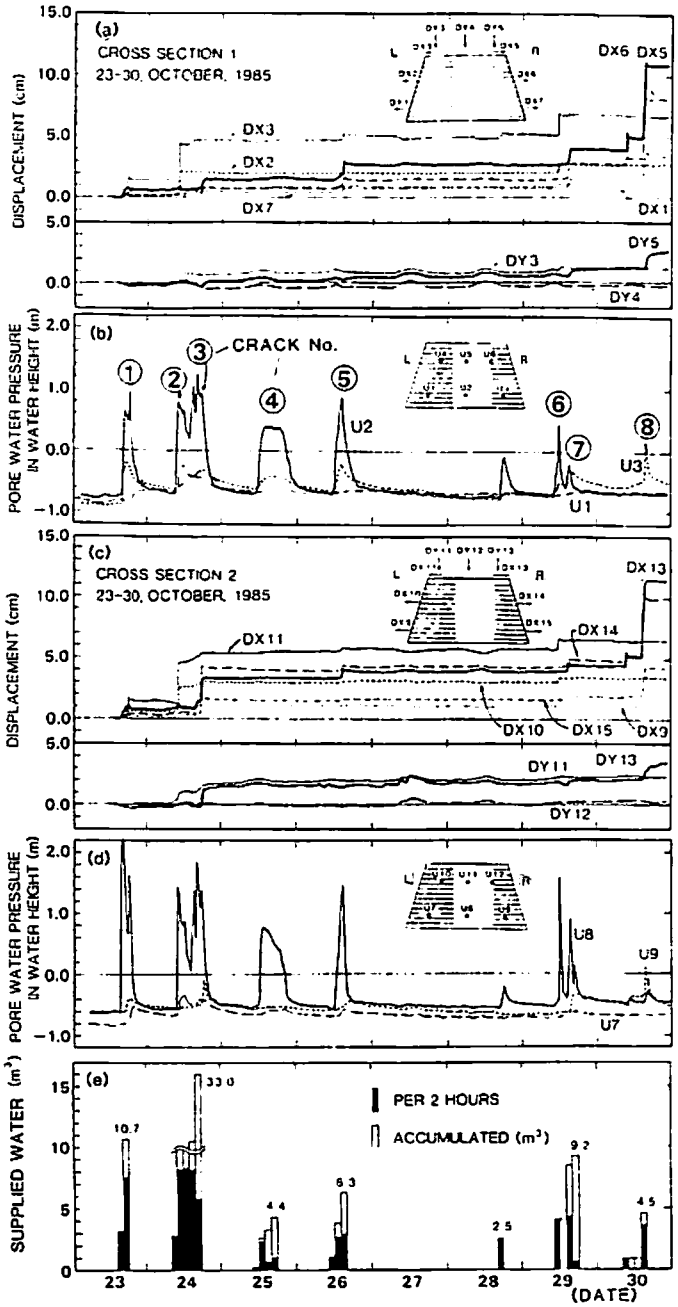

Fig.7.

Behavior of Embankment II during a period of water supply from the crest.

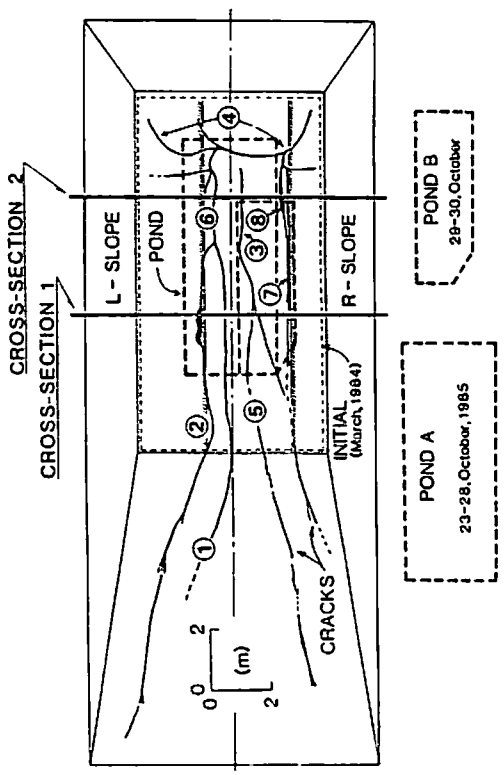

Fig.6. Ponds and cracks on the crest of Embankment II during a period of water supply from the crest.

pullout resistance/the tensile strength" is very large, since non-woven geotextile sheets have much larger contact area with soil and have lower tensile strengths. Consequently, the anchoring length required to activate the pull-out resistance comparable with the tensile strength is much smaller for the non-woven geotextiles.

(b) In many present design methods of reinforcing steep slopes, it is assumed that a horizontal earth pressure P_i, acting to each soil layer which involves a layer of reinforcement i as shown in Fig.5a, is resisted by the tensile force T_i working in the reinforcement i at the intersection between the slip surface and the reinforcement i ((5) among others). This implies that the shear stresses working on the horizontal surfaces $\overline{ac}$ and $\overline{bd}$ are neglected. Such an idea of "independent horizontal equilibrim for each soil layer" as above can be considered as a safe-side idea. If the contribution of the shear stress on the horizontal surfaces to the overall stability of the slope is taken into account, the length of reinforcements can be made smaller without losing the overall stability. In this case, at the higher levels some reinforcements may not extend beyond the critical slip surface as illustrated in Fig.5b. The overall bending rigidity of the face structure, if it has, will decreases the shear deformation of the slope caused by the shear stresses working on the horizontal surfaces.

It will be shown later in this paper and in the companion paper (3) that the slope reinforced with short geotextile sheets can be stable, whereas the possibility of overturning about a point on the face, usually about the toe of the slope, increases. To prevent overturning, the soil next to the face should have a large resistance against local compression.

3. BEHAVIOR OF TEST EMBANKMENTS

In the second year after the construction, the slopes of Embankment II did not show any noticeable displacements (refer to (1), (2)). Considering that the slopes will not show noticeable displacements any more even under natural heavy rainfall in future, a supply of about $70m^3$ of water was allowed to percolate through from its crest over a period of eight days from 23 through 30, October 1985 (Fig.6). By the noon in 29 October, water was supplied from Pond A located at the center of the crest. Several large cracks appeared behind the back end of the left-hand reinforced zone as designated by ① and ② in Fig.6. The numbers in the circles represent the sequences of appearance of cracks on the crest. Pond A was located above the back face of the reinforced zone in the left-hand slope, but not above that of the right-hand slope. Since major cracks tended to appear in the

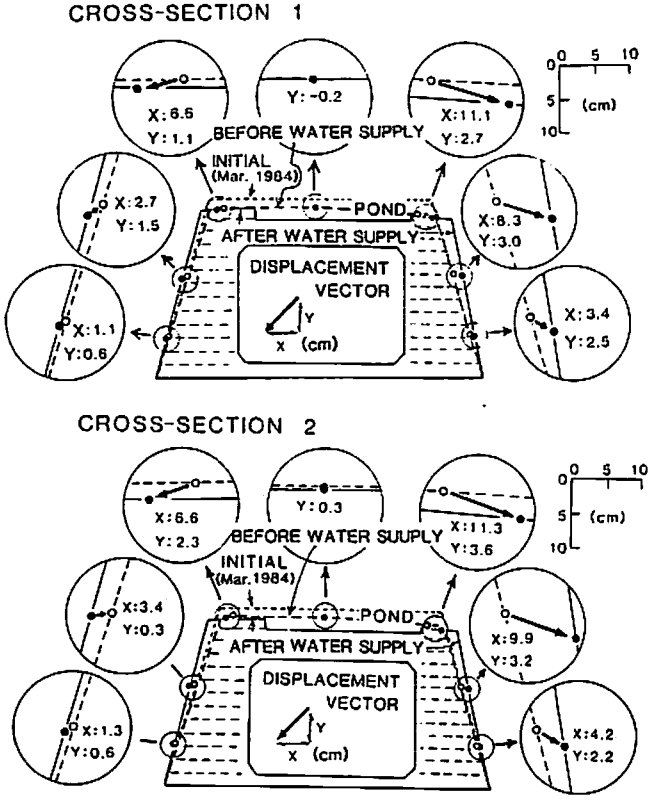

Fig.8. Deformation of Embankment Ⅱ by water supply from the crest.

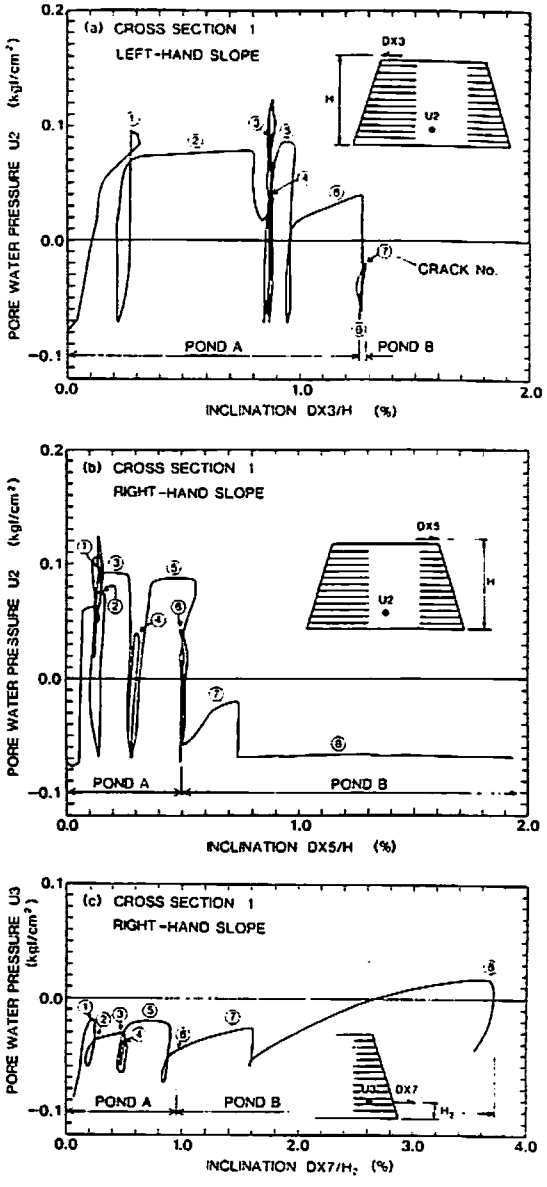

Fig.9.

Relationships between slope face inclination and pore water pressure for Embankment Ⅱ observed during a period of water supply.

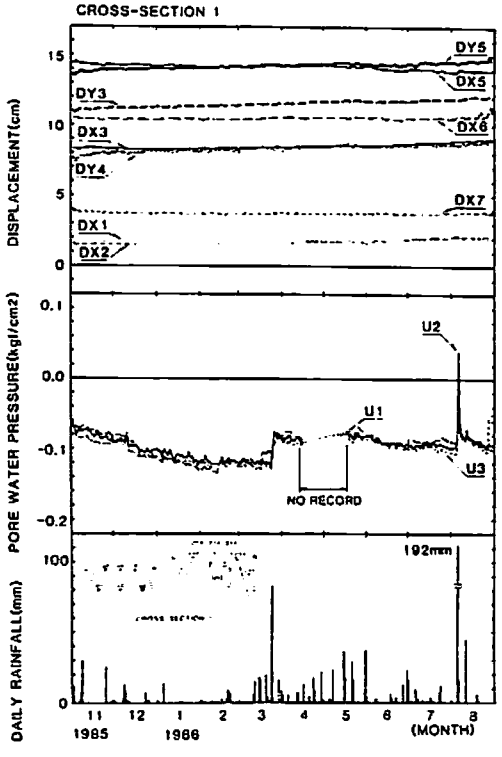

Fig.10. Behavior of Embankment Ⅱ after water supply from the crest.

unreinforced zone adjacent to the back face of the reinforced zone, most of water flew into the cracks ①and ②. Therefore, the left-hand slope displaced more than the right-hand slope, despite the length of geotextile was larger in the left-hand slope than in the right-hand slope (Fig.7). After the noon in 29, water was supplied from Pond B which had been made closer to the right-hand slope, so that Pond B was located above the back face of the reinforced zone in the right-hand slope. As a consequence, other cracks as designated by ⑦ and ⑧ appeared behind the back face of the right-hand reinforced zone. Associated with the flowing of water into the cracks ⑦ and ⑧, the right-hand slope displaced noticeably. The total displacement during this period (i.e., eight days) at representative points are shown in Fig.8, which was larger in the right-hand slope than in the left-hand slope. In Fig.8, the rotational displacement about the toe of the slopes can be clearly seen.

It may be seen from Fig.7 that the increase in pore water pressure was much smaller in the reinforced zones than in the central unreinforced zone. This behavior can be attributed to the following two reasons; (a) rapid drainage of water in the reinforced zones through the geotextile, and (b) vertical cracks appeared only in the unreinforced zones, but not in the reinforced zones.

Fig.9 shows the relationship between the pore water pressure and the inclination of slope face, the magnitude of which represents the degree of the instability of the slope. It may be seen that the behavior has an elasto-plastic property in such that the increase in pore water pressure acts as an increase in load to the slope; i.e., the increase in pore water pressure results in (a) the decrease in the shear strength of soil and (b) the increase in horizontal load to the slope. It may be seen from Fig.9(a) that the outwards displacement of the left-hand slope is closely related to the increase in the pore water pressure U2. The outward displacement of the right-hand slope is not well related to the increase in the pore water pressure U2 (Fig.9b), but is very closely related to the increase in the pore water pressure U3 (Fig.9c), since in the right-hand slope a shear zone passes through near the point U3 as shown in Fig.11.

After filling the cracks with a slurry of slaked lime, the long-term observation was started again (Fig.10). It may be seen that in spite of relatively large deformations experienced during the water supply from the crest, the deformation of Embankment Ⅱ in the subsequent year was very small.

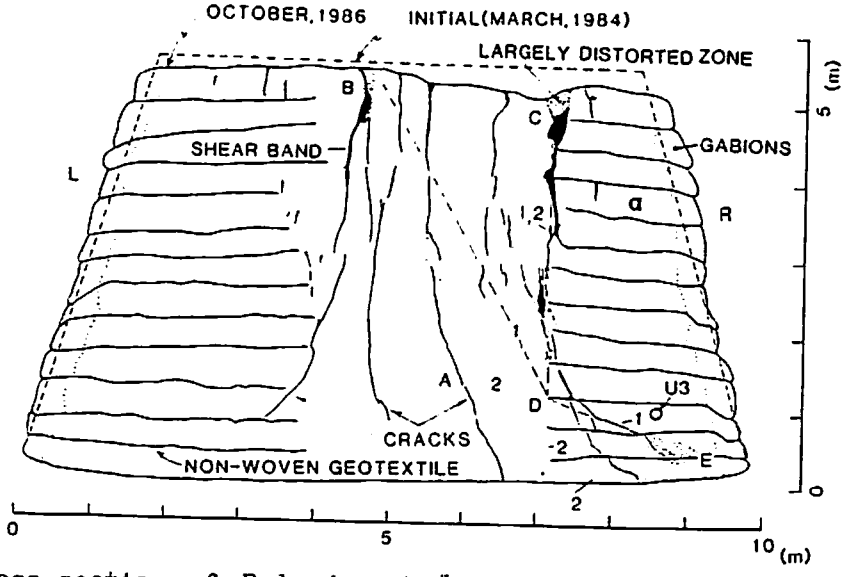

Fig.11. Cross-section of Embankment Ⅱ observed at dismantling. 1: Failure surface by analysis with no water pressure in cracks, 2: Failure surface by analysis with water pressure in cracks.

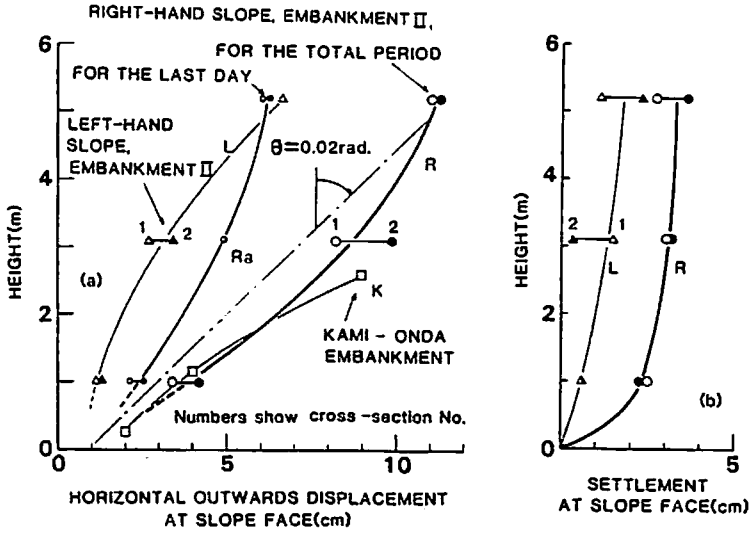

Fig.12. Relationships between either (a) horizontal outwards displacement, or (b) settlement, and slope height at slope faces observed during water supply from the crest or artificial rainfall.

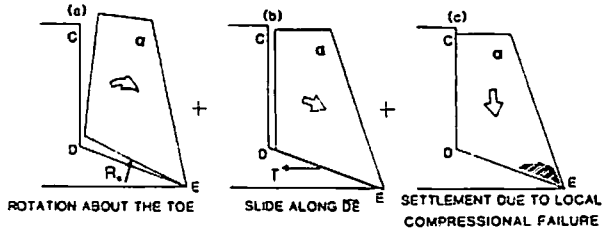

Fig.13. Schematic diagram showing deformation of right-hand slope of Embankment Ⅱ.

Fig.11 shows the cross-section exposed at the dismantling of Embankmen Ⅱ. The following points were learned from this observation:

(1) There exist both tension cracks and shear bands. Tension cracks, oriente in the direction of the maximum compressive principal stress, had a smal width of the order of several mm to several cm, as typically seen at Poin A. Shear bands, associated with the shear failure of the soil, had relatively large width of the order of 10cm or more. In each slope, a shea band starts from the crest (Points B or C) and becomes less clear at deepe places. At Point D, the direction changes from the vertical to the incline direction oriented toward the toe (Point E).

(2) Tension cracks and shear bands appeared only in the unreinforced zon except near the toe of the right-hand slope. In particular, near the crest a clear contrast as to the development of tension cracks and shear band may be seen between the unreinforced and reinforced zones. Therefore, i seems that in the reinforced zones, the percolation of water from the cres through cracks and shear bands were effectively prevented.

(3) Near the slope faces where manual tamping was used, the compression o soil was larger, probably due to a low efficiency of manual tamping.

(4) The curves L and R shown in Fig.12a represent the relationships betwee the total horizontal outwards displacement at the slope faces by th eight-day water supply and the height for the left-hand and right-han slopes of Embankment Ⅱ, whereas the curve R_a represents the displacemen of the right-hand slope face in the last one day of the eight days, induce by the water supply from Pond B (Fig.6). The curve K represents th horizontal displacement at the slope face of Kami-Onda Embankment by th four-day artificial rainfall (3). The curves L and R shown in Fig.12 represent the relationships between the total vertical displacemen (settlement) and the height at the left-hand and right-hand slope faces o Embankment Ⅱ, corresponding to the curves L and R in Fig.12a. From Figs 1 and 12, it is considered that the following three different modes o deformation took place; namely,

(1) Rotation about the toe: For Embankment Ⅱ, the rotational displacemen was larger in the right-hand slope than in the left-hand slope, yet th right-hand slope did not lose its overall stability. The rotational displacement of the slope face was also large for Kami-onda Embankment As schematically shown in Fig.13a (see also Fig.11), the reinforced zone c rotated about the toe like a monolith, associating shear bands $\overline{CD}$ and $\overline{DE}$ and many vertical tension cracks in the unreinforced zone behind the

reinforced zone α, and also associating a depression at the crest between Points B and C.

(ii) Sliding along a shear band: In Fig.12a, the positive intersections of the curves at the horizontal axis indicate that the horizontal outward sliding took place too. In the right-hand slope of Embankment Ⅱ, this took place along the plane $\overline{DE}$ (see Figs 11 and 13b). It may also be seen from Figs9 b and c that the inclination at the right-hand face at the stages ⑦, ⑧ caused by the water supply from Pond B are as follows; at the crest, DX5/H=1.4% and at the height H_2=1.2m, DX7/H_2=2.8%. This means that this displacement at the slope face was not purely rotational, but included a displacement by horizontal sliding.

(iii) Local compression near the toe: Only by the rotation and horizontal sliding, such settlements at the slope face as shown in Fig.12b could not take place. It seems that the compression of soil near the slope surface, especially near the toe, took place associated with stress concentration induced by the increased overturning moment (Fig.13c). This implies that in order to prevent a larger rotational displacement, it is very effective that near the face, in particular near the toe, (a) the soil is well compacted and/or imcompressive granular materials are used, and (b) the horizontal confinement to the soil is provided by face structures such as gabions or concrete panels or others. In other words, the location of reaction as designated by R_a in Figs 13a and 14c is moved closer to the slope face by increasing the rigidity and strength of the soil near the slope face, and thereby the safety factor against overturning is increased.

It is clear that in the slopes of Embankment Ⅱ and Kami-onda Embankment, the displacement due to the rotational mode was the largest among the above three modes.

Summarizing the behavior of the test embankments, it has been realized that the following three failure modes, as schematically shown in Fig.13, should be analysed in designing steep clay slopes; i.e., (i) overturning, especially when short geotextile sheets are used, (ii) sliding, for any length of geotextile, and (iii) local compressive failure of soil, especially when the soil is soft as Kanto loam. The last term was analysed by the FEM and the result is reported elsewhere (6).

4. STABILITY ANALYSIS FOR EMBANKMENT Ⅱ

The overall stability for overturning and sliding of the slopes of embankment Ⅱ was examined based on a two-wedge failure mechanism (5) (Fig.14). In the analysis, a soil-geotextile friction angle φ_μ of 30° and the tensile

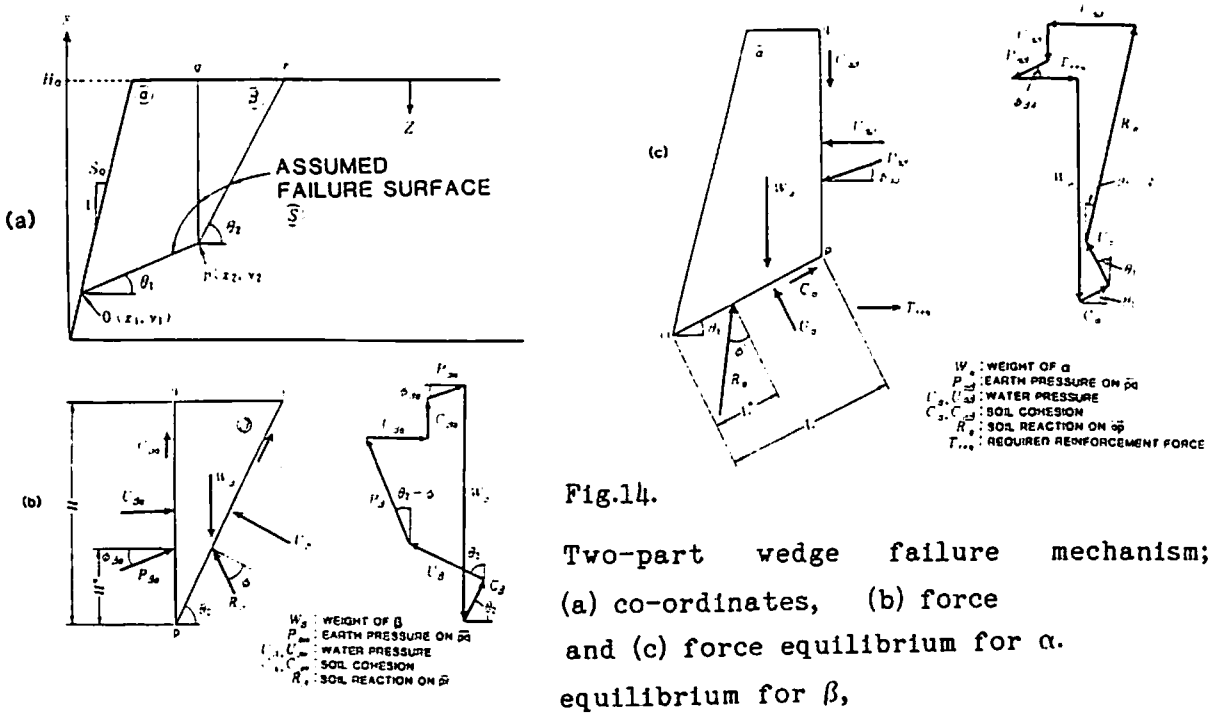

Fig.14.

Two-part wedge failure mechanism; (a) co-ordinates, (b) force and (c) force equilibrium for α. equilibrium for β,

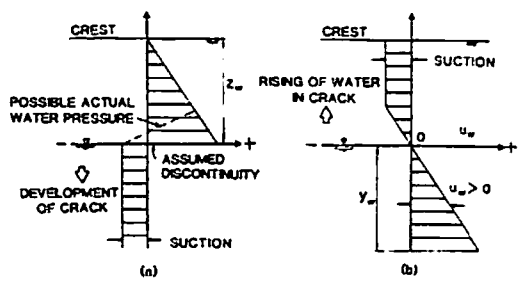

Fig.15.

Two distributions of water pressure in crack assumed in the analysis.

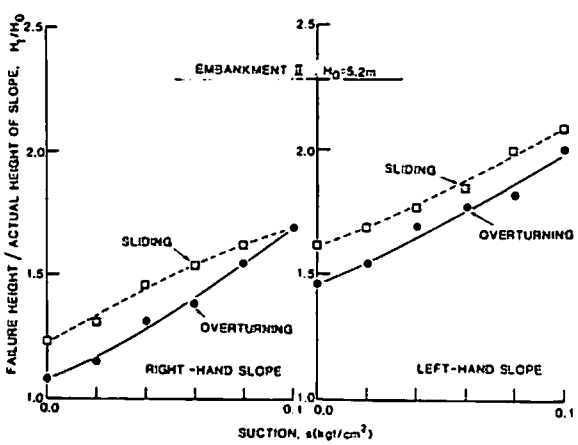

Fig.16.

Safety factors of slopes of Embankment II with no water pressures in cracks.

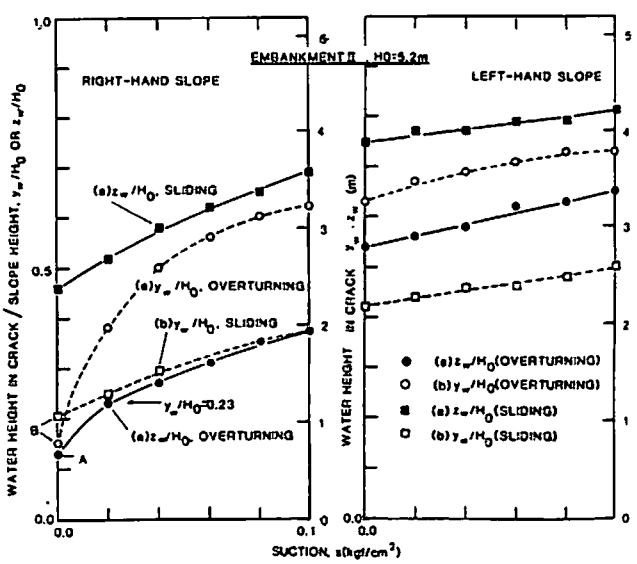

Fig.17.

Safety factors of slopes of Embankment II with water pressures developed in cracks.

strength of the geotextile α_f given in Table 2 were used. It was taken into account that for a length of 1.7m from the face, the geotextile sheets were overlapped, thus the tensile strength is $2\alpha_f$ (this was not considered in the previous paper (2)). The soil friction angle $\varphi_{\alpha\beta}$ along the vertical surface $\overline{pq}$ (Fig.14) was ignored when the surface $\overline{pq}$ is located outside the reinforced zone, but $\varphi_{\alpha\beta}=30°$ (equal to the effective angle of internal friction of the soil φ') was used when the surface $\overline{pq}$ is located inside the reinforced zone. The angle $\varphi_{\alpha\beta}$ has a large effect on the computed safety factor against overturning; i.e., a larger safety factor for a larger $\varphi_{\alpha\beta}$. The above assumption was made considering that the reinforced zone has a larger resistance against the development of vertical cracks. The earth pressure $P_{\alpha\beta}$ was assumed to act at a height of $\overline{pq}/3$ from the point p.

The reaction R_α of soil on the surface $\overline{op}$ was assumed to act at a distant of $\overline{op}/3$ from the point o. The location R_α has a large effect on the computed safety factor against overturning; i.e., the closer to the point o the reaction point is, the larger the safety factor.

The gross required tensile reinforcement force (T_{req}) and the gross required resistance against overturning (M_{req}) are defined as the additional horizontal force and moment required for the assumed failure mechanism; therefore, T_{req} and M_{req} are a function of the coordinates of the points o and p and the angles θ_1 and θ_2. The gross tensile reinforcement force (T_{avail}) and moment (M_{avail}) avalable for the assumed failure mechanism are given by

$$T_{avail}=\sum(T_{avail})_i,\ M_{avail}=\sum l_i\times(T_{avail})_i,\quad (T_{avail})_i=\min[(\alpha_f)_i,(T_A)_i] \tag{1}$$

where $(T_{avail})_i$ is the tensile force available for each layer of reinforcement, l_i is the height of the ith reinforcement layer from the point o, $(\alpha_f)_i$ is the tensile strength of the ith reinforcement layer and $(T_A)_i$ is the pull-out resistance for the ith reinforcement layer having a length $(L_A)_i$ extending behind the failure surface $\overline{op}$ or $\overline{pq}$, which is given by $(T_A)_i = 2\gamma_t\cdot z_i\cdot \tan\varphi_\mu\cdot(L_A)_i$. It is to be noted that $(L_A)_i$ for satisfying that $(T_A)_i = (\alpha_f)_i$ is small; for a single geotextile sheet, even at z_i=4m, L_{Ai} is about 15cm. A soil unit weight γ_t=1.34tf/m^3(13.1kN/m^3) was used. The safety factor SF is defined as $\min(T_{avail}/T_{req})$ for sliding failure and $\min(M_{avail}/M_{req})$ for overturning for all possible failure mechanisms. Note that in this analysis, some geotextile sheets located at higher levels may not extented beyond the failure surface even when the overall safety factor is larger than 1.0 as illustrated in Fig.5b.

The effect of rainfall was taken into account in the following two

simplified ways; i.e.,(a) as a reduction of the negative pore water pressure (suction, s), (b) as a positive water pressure in vertical cracks and the same water pressure in the soil at the same level as illustrated in Fig.15. The water pressure distribution (a) shown in Fig.15 simulates a crack which is developing from the crest down to a certain depth z_w, filled with water. For simplicity, a discontinuous distribution in water pressure was assumed, whereas in the true distribution it is continuous as represented by the broken line. The water pressure distribution (b) simulates water pressure in a crack which has developed for the whole height of the embankment and is filled partially with water up to a certain height y_w.

The shear strength of the soil was given by

$$\tau_f=(\sigma+s)\cdot\tan\phi' \quad \text{when } s>0 \text{ or } u_w<0, \qquad \tau_f=(\sigma-u_w)\cdot\tan\phi' \quad \text{when } u_w>0 \qquad (2)$$

where σ is the total normal stress, s is the suction and u_w is the pore water pressure. The strength parameter $\phi'=30°$ was selected (1), (2).

The failure height H_f was defined as the height of slope when SF becomes 1.0 when unchanging the horizontal location of the truncated end of geotextile layers. Fig.16 shows the ratio of H_f to the actual embankment height H_0=5.2m as a function of the suction s, where the water pressure in cracks are ignored. The following points may be seen;

(1) The safety factor (i.e., H_f/H_0) is lower against overturning than against sliding. This is a characteristic feature for short geotextiles. This result seems to be well in accordance with the actual behavior.

(2) The safety factor is much smaller for the right-hand slope having shorter geotextile sheets than for the left-hand slope having longer geotextile sheets, as actually observed both during a series of natural heavy rainfall and during a period of water supply from the crest.

(3) The effect of the suction s on the computed safety factor is considerable. This result clearly indicates the importance of the ability of the reinforcement to drain such clay slopes in order to maintain as high as possible the suction.

(4) The critical slip surface when s=0 in the right-hand slope is indicated by broken lines 1 in Fig.11. A very good coincidence with the actural failure surface may be seen.

Fig.17 shows either the level of water in crack in terms of z_w for the water pressure distribution (a) or that in terms of y_w for the water pressure distribution (b) when SF is 1.0. The following points may be seen;

(1) For sliding, the safety factor in terms of y_w/H_0 for the water pressure distribution (b) is smaller than that in terms of z_w/H_0 for the distribution

(a), since for the distribution (b), the water pressure U_n acting on the slip surface $\overline{op}$ (see Fig.14c) reduces considerably the shear resistance of soil.
(2) For overturning, the safety factor in terms of z_w/H_0 for the distribution (a) is smaller than that in terms of y_w/H_0 for the distribution (b), since for the distribution (a) the water pressure $U_{n\beta}$ acting on the vertical slip surface $\overline{pq}$ (see Fig.14c) increases considerably the overturning moment.
(3) The displacement of the right-hand slope during the eight-day water supply may be explained as follows. First, the water pressure distribution (a) appeared as vertical cracks developed from the crest, and the safety factor against overturning becomes so small, as indicated by the letter A in Fig.17 (s=0 is assumed), that vertical cracks developed deeper, even down to the bottom of the embankment, associated with the rotational displacement. Then, the water pressure distribution (b) appeared. At the stage 8 (see Figs 7 and 9c), the water pressure U3 is about 0.2m; i.e., y_w=1.0m+0.2m=1.2m and y_w/H_0=0.23. This implies that both sliding and overturning can take place as indicated by the points denoted by B in Fig.17 (s=0 is assumed).
(4) The critical slip surface in the right-hand slope when the water pressure in cracks is taken into account is indicated by dotted lines 2 in Fig.11. These are somewhat different from the actual ones, especially near the toe. However, the general pattern is very similar.

5. CONCLUSIONS

Four clay test embankments reinforced with a non-woven geotextile were constructed. It was found that non-woven geotextile sheets are very useful for allowing better compaction, draining pore water from the interior of embankments and tensile soil reinforcement. The last term includes the prevention of developing vertical cracks, which can be easily developed when the embankment is not reinforced. The pore water in cracks reduces the soil strength and increases a horizontal load to the slope.

It was shown that steep clay slopes reinforced with relatively short geotextile sheets can be sufficiently stable even during heavy rainfall, while overturning is easier to occur than sliding when compared with the case where longer geotextile sheets are used. It was also shown that the face structure is essencial for steep clay embankment for preventing the local compressional failure of the soil near the slope face and associated sliding failure and overturning.

A simplified method of stability analysis by the limit equilibrium method, which can explain, at least qualitatively, the actual behavior of

the embankments, has been presented. In this method, it is considered that the slope is stable when the overall safety factor is large enough even if some geotextile sheets located at higher levels do not extend beyond the failure surface.

6. ACKNOWLEDGEMENTS

The authors with to thank Mr. S. Yamamoto and Mr. H. Kuwabara of Tokyo Electronic Power Co., and our colleagues, Mr. T. Sato, Mr. S. Yamada and Miss M. Torimitsu for their co-operation in this study. This study was partly sponsored by the Ministry of Education and Culture of the Japanese Government.

7. REFERENCES

1. Tatsuoka, F., Yamauchi(Ando), H., Iwasaki, K. and Nakamura, K., "Performance of Clay Test Embankments Reinforced with a Non-Woven Geotextile," Proc. 3rd Int. Conf. Geotexiles, Wien, Vol.Ⅱ, pp.355-360. 1986.
2. Tatsuoka, F. and Yamauchi, H. (1986), "A Reinforcing Method for Steep Clay Slopes Using a Non-Woven Geotextile," Geotextiles and Geomembranes, 4, pp.241-268, 1986.
3. Tatsuoka, F., Nakamura, K., Iwasaki, K., Tamura, Y., and Yamauchi, H. "Behavior of Sreep Clay Embankments Reinforced with a Non-Woven Geotextile Having Various Face Structure", Proc. of the Post Vienna Conf. on Geotextiles, Singapore, 1987.
4. Iwasaki, K., Kiyokawa, N., Ishida, K., Kato, T. and Nishimura, J., "Endurance Property of a Non-Woven Geotextile Used for Drainage System and Reinforcing in the Steep Slope Embankment," Proc. 22 Japanese Sym. on SMFE, Niigata, Vol.2, pp.1757-1758, 1986 (in Japanese).
5. Jewell, R. A., Paine, N. and Woods, R. I., "Design Methods for Steep Reinforced Embankments," Proc. Symp. Polymer Grid Reinforcement in Civil Engng, London, Paper No.31, London, 1984.
6. Yamauchi, H., "A Method of Reinforcing Clay Embankments with a Non-Woven Geotextile," Dr. of Engng, Thesis, Univ. of Tokyo, 1986 (in Japanese).